Composition, Architecture, and Functional Implications of the Connective Tissue Network of the Extraocular Muscles

Linda K. McLoon,[1] André Vicente,[2] Krysta R. Fitzpatrick,[1] Mona Lindström,[3] and Fatima Pedrosa Domellöf[2,3]

[1]Department of Ophthalmology and Visual Neurosciences, University of Minnesota, Minneapolis, Minnesota, United States
[2]Department of Clinical Science, Ophthalmology, Umeå University, Umeå, Sweden
[3]Department of Integrative Medical Biology, Anatomy, Umeå University, Umeå, Sweden

Correspondence: Fatima Pedrosa Domellöf, Department of Clinical Science, Ophthalmology, Umeå University, Umeå 90185, Sweden; fatima.pedrosa-domellof@umu.se.

Submitted: September 18, 2017
Accepted: December 3, 2017

Citation: McLoon LK, Vicente A, Fitzpatrick KR, Linström M, Pedrosa Domellöf F. Composition, architecture, and functional implications of the connective tissue network of the extraocular muscles. *Invest Ophthalmol Vis Sci*. 2018;59:322–329. https://doi.org/10.1167/iovs.17-23003

Purpose. We examined the pattern and extent of connective tissue distribution in the extraocular muscles (EOMs) and determined the ability of the interconnected connective tissues to disseminate force laterally.

Methods. Human EOMs were examined for collagens I, III, IV, and VI; fibronectin; laminin; and elastin using immunohistochemistry. Connective tissue distribution was examined with scanning electron microscopy. Rabbit EOMs were examined for levels of force transmission longitudinally and transversely using in vitro force assessment.

Results. Collagens I, III, and VI localized to the endomysium, perimysium, and epimysium. Collagen IV, fibronectin, and laminin localized to the basal lamina surrounding all myofibers. All collagens localized similarly in the orbital and global layers throughout the muscle length. Elastin had the most irregular pattern and ran longitudinally and circumferentially throughout the length of all EOMs. Scanning electron microscopy showed these elements to be extensively interconnected, from endomysium through the perimysium to the epimysium surrounding the whole muscle. In vitro physiology demonstrated force generation in the lateral dimension, presumably through myofascial transmission, which was always proportional to the force generated in the longitudinally oriented muscles.

Conclusions. A striking connective tissue matrix interconnects all the myofibers and extends, via perimysial connections, to the epimysium. These interconnections are significant and allow measurable force transmission laterally as well as longitudinally, suggesting that they may contribute to the nonlinear force summation seen in motor unit recording studies. This provides strong evidence that separate compartmental movements are unlikely as no region is independent of the rest of the muscle.

Keywords: extraocular muscles, connective tissue, collagen, muscle force, scanning electron microscopy, perimysium, epimysium

The extraocular muscles (EOMs) have complex microscopic anatomy and physiological properties. They are composed of two distinct layers, an orbital layer with myofibers that have a small mean cross-sectional area and a global layer in which the mean cross-sectional areas are larger than in the orbital layer but still significantly smaller than in limb muscles.[1,2] In addition, the myofibers are short and do not run the full length of the muscles.[3–5] The myofibers in EOMs are loosely arranged and separated by an extensive extracellular matrix, with greater complexity and molecular diversity of connective tissue matrix components than seen in limb skeletal muscles.[6,7] This is manifested by specific differences in laminins[7] and differences in the properties of fibroblasts compared to limb skeletal muscle.[8] These differences are significant, and play a role in differences in their disease profile.[9,10]

The connective tissue in skeletal muscles is typically subdivided into three levels: the endomysium, which forms an ensheathment surrounding the individual muscle fibers; the perimysium, which surrounds groups of muscle fibers, forming muscle fiber bundles; and the epimysium, which surrounds the whole muscle. The muscle connective tissue is interconnected both circumferentially and longitudinally from the endomysium to the epimysium[11,12] and is critically important in determining the overall mechanical properties of the whole muscle.[13] It has been long known that during limb muscle contraction force is not only transmitted to the fibrous tendons at the muscle insertion but also is transmitted laterally through endomysial, perimysial, and epimysial radial connections.[12,14,15] Taken together, the muscle connective tissue components, along with the tendon, form a functional link between the muscle fibers and the bone. Lateral transmission of force is considered to be particularly significant in muscles where myofibers do not run the full muscle length.[14,16,17] In addition, this myofascial or lateral force transmission was shown to be increasingly important at lower forces.[18]

At the molecular level, the main component of intramuscular connective tissue is collagen, with collagen type IV, a network-forming collagen, present in the basement membrane of muscle fibers and the fibril-forming collagens type I and III dominating in the endomysium, perimysium, and epimysium, along with minor amounts of other collagen types, including collagen VI, a microfibril-forming collagen.[15,19–21] Additional

important extracellular matrix proteins in muscle are laminins and fibronectin, which are present in the basement membrane of muscle fibers, and elastin, the main structural protein responsible for tissue resilience and extensibility[22] and counteracting the stiffness provided by collagen.[23,24]

Recent studies have proposed that the EOMs, rather than acting in a unified manner, have compartments that move independently of each other. The first study posited that the orbital and global layers showed mechanical independence,[25] and the second series proposed that there were medial and lateral compartments within an extraocular muscle that functioned independently.[26,27] Based on the extensive literature supporting the interconnectedness of skeletal muscle in terms of its function, we performed a comprehensive examination of the connective tissue components in human and rabbit EOMs using three different methods to determine their composition, architecture, and lateral force transmission. We used immunohistochemical methods to visualize collagen types I, III, IV, and VI[28–30] as well as laminin, fibronectin, and elastin. Scanning electron microscopy was used to visualize the complete connective tissue matrix in the absence of muscle fibers.[31] Finally, the lateral dissipation of force of whole EOMs was measured using in vitro physiological methods.[14,16,17] Studies have suggested that there are compartments within the EOMs that move independently from each other[26,27]; the collective data in our study support the view that existence of separately acting compartments within EOMs are unlikely due to significant interconnectedness of collagens and other connective tissue elements between the orbital and global layers.

Methods

All studies were approved by the Regional Ethical Review Board in Umeå, the institutional review board for use of human tissues at the University of Minnesota, and by the Institutional Animal Care and Use Committee of the University of Minnesota, as well as the Swedish Board of Agriculture. All human tissue use conformed to the tenets of the Declaration of Helsinki, and all animal research conformed to the guidelines of the National Institutes of Health and the ARVO Statement for the Use of Animals in Ophthalmic and Vision Research.

The following human EOMs from seven subjects with a mean age of 68.3 years (range, 4–98), divided evenly between males and females, were processed for immunohistochemistry: medial rectus ($n = 5$), lateral rectus ($n = 2$), superior rectus ($n = 1$), and superior oblique ($n = 1$). The muscles were collected at autopsy, mounted on a piece of cardboard using OCT cryomount (HistoLab Products AB, Gothenburg, Sweden), and then snap-frozen in liquid propane chilled with liquid nitrogen. The samples were stored at −80°C until sectioning. Whole EOMs serial cross sections, 5 μm thick, were cut from the anterior, middle, and posterior portion of most samples, whereas in some cases not all three parts were available. The sections were collected on slides (Superfrost Plus; Thermo Fisher Scientific, Braunschweig, Germany) or gelatin-coated glass slides and stored at −20°C until processed for immunofluorescence, as previously described[10] using the following primary antibodies: mouse monoclonal antibody GTX26308 against type I collagen (1:5000; GeneTex, Irvine, CA, USA), rabbit polyclonal antibody ab7778 against collagen III (1:500, Abcam, Cambridge, UK), mouse monoclonal antibody M0785 against collagen IV (1:500; Dako, Glostrup, Denmark), mouse monoclonal antibody AF6210 COL6A1 against collagen VI (1:750; Acris Antibodies, Inc., Herford, Germany), sheep polyclonal antibody PC128 against human laminin (1:15,000; The Binding Site, Birmingham, UK), rabbit polyclonal antibody A0245 against human fibronectin (1:5000; DakoCytomation, Glostrup, Denmark), and mouse monoclonal antibody E4013 against elastin (1:2500; Sigma-Aldrich Corp., St. Louis, MO, USA). The antibodies against the different collagens are type specific, raised against nondenatured three-dimensional epitopes, and extensively purified to guarantee high specificity. The secondary antibodies were conjugated with Alexa Fluor 488 (Molecular Probes, Inc., Eugene, OR, USA) or Rhodamine Red-X (Jackson ImmunoResearch Europe Ltd., Newmarket, UK). For elastin, the slides were rinsed and incubated with the Vectastain horseradish peroxidase labeling kit. After rinsing in phosphate buffered saline, the sections were reacted with the heavy metal intensified diaminobenzidine procedure, dehydrated, and coverslipped for analysis. The sections were evaluated using a microscope (Nikon Eclipse E800; Nikon, Inc., Melville, NY, USA) equipped with a slider camera (SPOT RT KE; Diagnostic Instruments, Inc., Sterling Heights, MI, USA), and microscopes (Leica DM 6000 B, Leica DMR; Leica Microsystems, Wetzlar, Germany) equipped with digital high-speed fluorescence charge-coupled device cameras (Leica DFC360 FX; Leica Microsystems).

A human medial rectus muscle and rabbit medial rectus ($n = 6$), lateral rectus ($n = 10$), soleus ($n = 9$), and gastrocnemius ($n = 8$) muscles were prepared for scanning electron microscopy using a method that preserves the connective tissue but results in elimination of the myofibers contained within the tissue.[31] Excised muscles were stretched to their estimated original length and attached with needles to a cork plate, fixed in 2.5% glutaraldehyde in 0.2 M sodium cacodylate buffer at room temperature for 30 minutes. The muscle samples were then removed from the cork, divided along their length into smaller segments (e.g., anterior, middle, and posterior or more) comprising the whole-muscle cross section and further fixated overnight. The muscle fibers were removed from the fixed tissue by digestion in 10% (wt/vol) NaOH over a period of 4 to 6 days and maintained on a rocker. They were then rinsed in water, rinsed in 0.2 M cacodylate buffer, and treated with 1% osmium tetroxide in cacodylate buffer for 1 hour. They were then rinsed in cacodylate buffer, followed by dehydration in a graded series of ethanol and critical point drying. Thereafter, the tissues were mounted on aluminum holders and coated with gold/palladium in preparation for examination under a Carl Zeiss AG (Jena, Germany) Merlin Field Emission Scanning Electron Microscope (FESEM) with SmartSEM V.5.05 software at the Umeå Core Facility for Electron Microscopy at Umeå University.

Force production was measured using our in vitro force assessment system (Aurora Scientific, Aurora, Ontario, Canada) with small modifications. Paired superior rectus muscles were removed from the sclera to the apex of the orbit from four rabbits after euthanasia. The muscles were placed in a bath containing Ringer's solution maintained at 32°C with constant oxygenation. All epimysium was left intact. One randomly selected superior rectus muscle was tied at the origin and insertion using a 4.0 silk suture. These were attached to a stationary bar on one side and a lever arm on the other side and were lowered into a bath with Ringer's solution maintained at 32°C with constant oxygenation. In a second bath, the second muscle was oriented so that the lateral and medial sides, via sutures into the epimysium and muscle, were attached to the stationary bar on one side and the lever arm on the other side. Two electrodes flanked each of the muscle samples, which provided stimulation at 10, 20, 40, 100, 150, and 200 Hz, with 2 minutes of rest between each stimulation. The optimal preload was determined for each muscle. To determine lateral force, which is perpendicular to the orientation of the myofibers, the preload determined for the contralateral muscles was arbitrarily chosen as the preload for both sets of

Investigative Ophthalmology & Visual Science

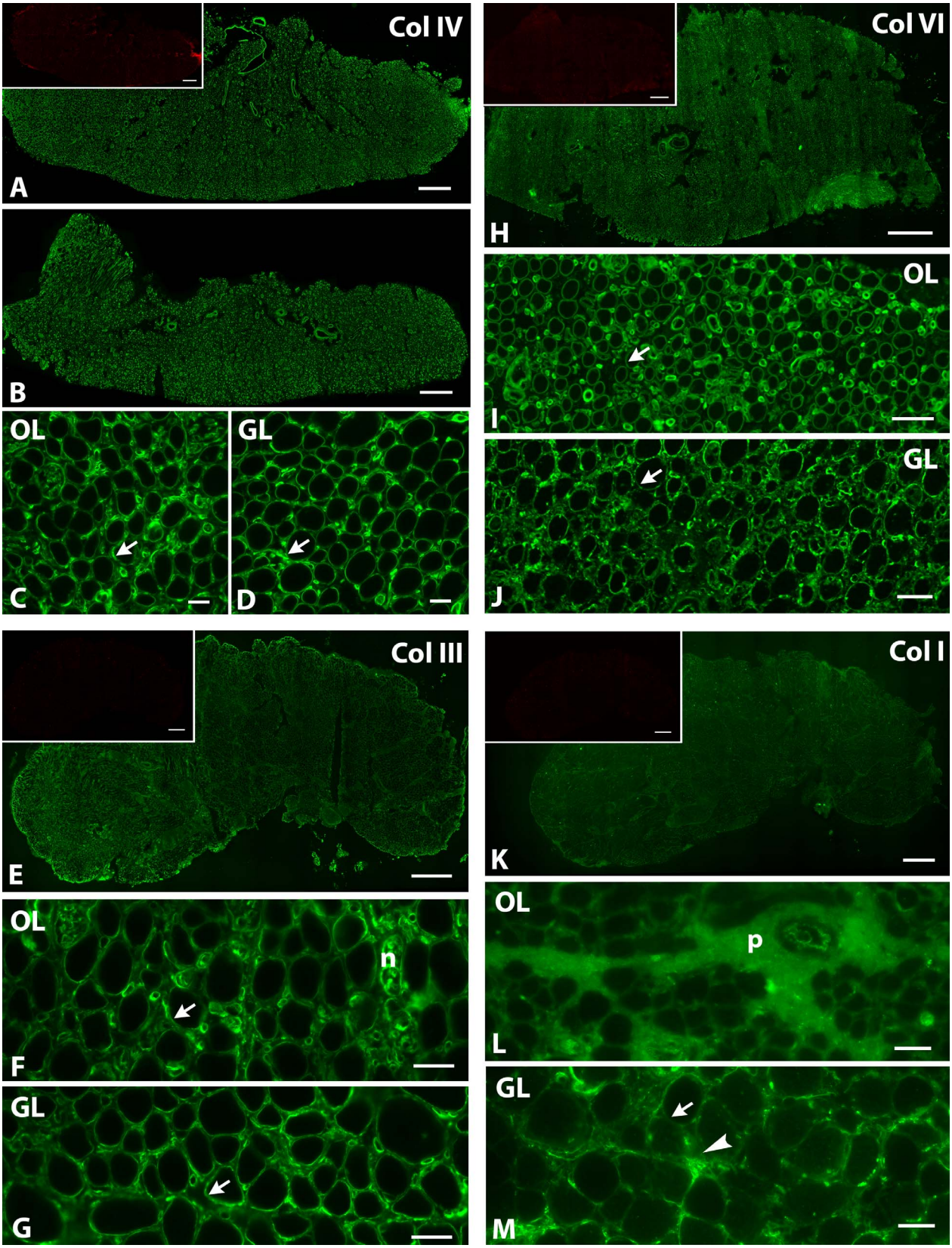

Figure 1. (**A–D**) Collagen IV immunostaining on a whole-muscle cross section of a medial rectus muscle cut at midbelly (**A**) and close to the tendon (**B**). Higher power photomicrographs of representative parts of the orbital layer (**C**) and global layer (**D**), showing uniform labeling of the fiber contours (*arrows*) throughout the muscle. (**E–G**) Collagen III immunostaining on a whole-muscle cross section of another medial rectus muscle cut at midbelly (**E**) and, at higher magnification, representative parts of the orbital layer (**F**) and global layer (**G**) showing strong labeling of the myofiber contours (*arrows*) and weak labeling of the interstitial space between them. Strong labeling of nerves (n) and vessels was also present.

Investigative Ophthalmology & Visual Science

(**H–J**) Collagen VI: whole-muscle cross section of a third medial rectus muscle cut at midbelly (**H**) and representative parts of the orbital layer (**I**) and global layer (**J**) shown at higher magnification. Notice that this antibody labeled the fiber contours (*arrows*) in a fragmentary pattern, particularly in the global layer (**J**), and it labeled both the perimysium and the epimysium (**H**). (**K–M**) Collagen I: whole-muscle cross section of a medial rectus muscle cut at midbelly (**K**) and representative parts of the orbital layer (**L**) and global layer (**M**) shown at higher magnification. This antibody labeled all connective tissue parts of the EOMs, even though with a more amorphous appearance (*arrow* indicates fiber contour; *arrowhead*, interstitial space; *p*, perimysium). The background staining level (*red*) for each whole-muscle section is shown in the corresponding insert in **A**, **E**, **H**, and **K**. It is important to note that all antibodies showed uniform staining patterns, with no differences within each EOM. *Scale bars*: 500 μm (**A**, **B**, **E**, **H**, **K**), 25 μm (**C**, **D**, **F**, **G**, **L**, **M**), and 50 μm (**I**, **J**).

muscles. Force was recorded in grams and also converted to millinewtons (mN) per square centimeter after taking mass and length measurements.[32] The forces generated at each stimulation frequency were averaged, and the separate means for the stimulated muscles in the longitudinally and laterally oriented muscle specimens were compared statistically using a paired *t*-test, with $P \leq 0.05$ considered statistically significant.

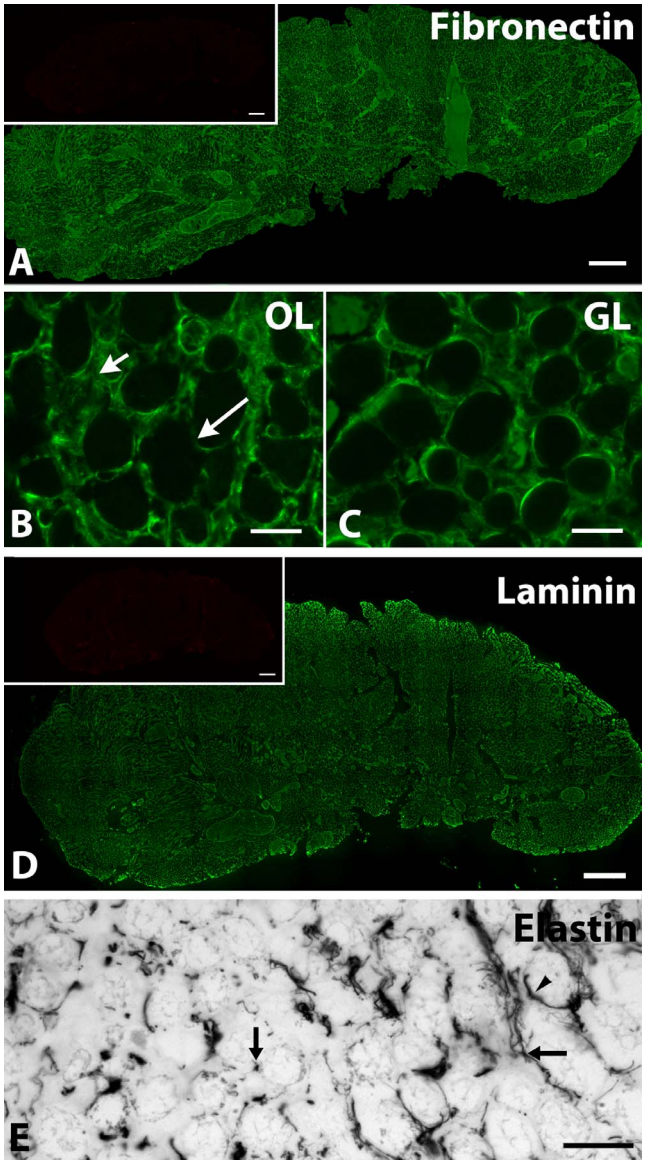

Figure 2. (**A–C**) Whole medial rectus muscle cross section taken at midbelly (**A**) and representative parts of the orbital (**B**) and global (**C**) layers showing uniform labeling of the fiber contours (*long arrow*) and the interstitial space between them (*short arrow*) with the antibody against fibronectin. The antibody against laminin (**D**) labeled the fiber contours, nerves, and vessels strongly. The background staining level (*red*) for each whole-muscle section is shown in the corresponding insert in **A** and **D**. Elastin fibers (**E**) were present in an irregular pattern, surrounding myofibers (*arrowhead*) and between myofibers (*arrows*). *Scale bars*: 500 μm (**A**, **D**), 25 μm (**B**, **C**, **E**).

Results

Connective Tissue Composition

The antibody against collagen IV clearly delineated the basement membrane surrounding all myofibers in the EOMs, both in the orbital and the global layers, with no differences along the length of the muscles (Fig. 1A–D). This antibody did not label the interstitial space between myofibers, the perimysium, or the epimysium, but it labeled the basement membranes of nerves and blood vessels (Fig. 1A–D).

The antibody to collagen III strongly labeled the basement membranes of all myofibers in both the orbital and global layers (Fig. 1E–G). In addition, faint immunostaining with collagen III could be seen in the perimysial connective tissue. Similar to the pattern of antibody staining for collagen IV, no differences were seen along the length of the muscles. Weak to moderate labeling with the antibody to collagen III was present in the epimysium (Fig. 1E). The connective tissue around the blood vessels and nerves was also labeled with this antibody (Fig. 1F).

Moderate to strong labeling with the antibody to collagen VI was evident in the endomysium, both in the basement membrane of myofibers and in the interstitial space between them, in the perimysium, and extended all the way to the epimysium, with no differences along the length of the muscles or between layers (Fig. 1H–J). This antibody also labeled the connective tissue around the blood vessels and nerves.

Strong staining with the antibody to collagen I was present in the perimysium and the epimysium (Fig. 1K–M). It was generally less dense in the endomysium, where it delineated the myofiber contours and filled the interstitial space between the muscle fibers. The labeling pattern of collagen I had an amorphous appearance and differed from the more fibrillar appearance seen in the staining with the antibodies to collagens III, IV, and VI. No differences in immunostaining patterns were observed between layers or along the length of the EOMs.

The antibody against fibronectin labeled the endomysium (Fig. 2A–C) with no differences in staining intensity between the orbital and global layers or along the length of the muscles. Fibronectin also labeled blood vessels and nerves.

The antibody against laminin labeled the basement membranes of the myofibers (Fig. 2D). This staining was similar along the length of the muscles and was equally strong in both the orbital and global layers, even though the smaller size of the muscle fibers in the orbital layer gave the general impression that there was higher staining intensity in this layer. Laminin did not immunostain the perimysium or epimysium, but it labeled the blood vessels and nerves strongly.

The antibody against elastin showed a complex distribution pattern (Fig. 2E). Elastin fibrils were found surrounding

Investigative Ophthalmology & Visual Science

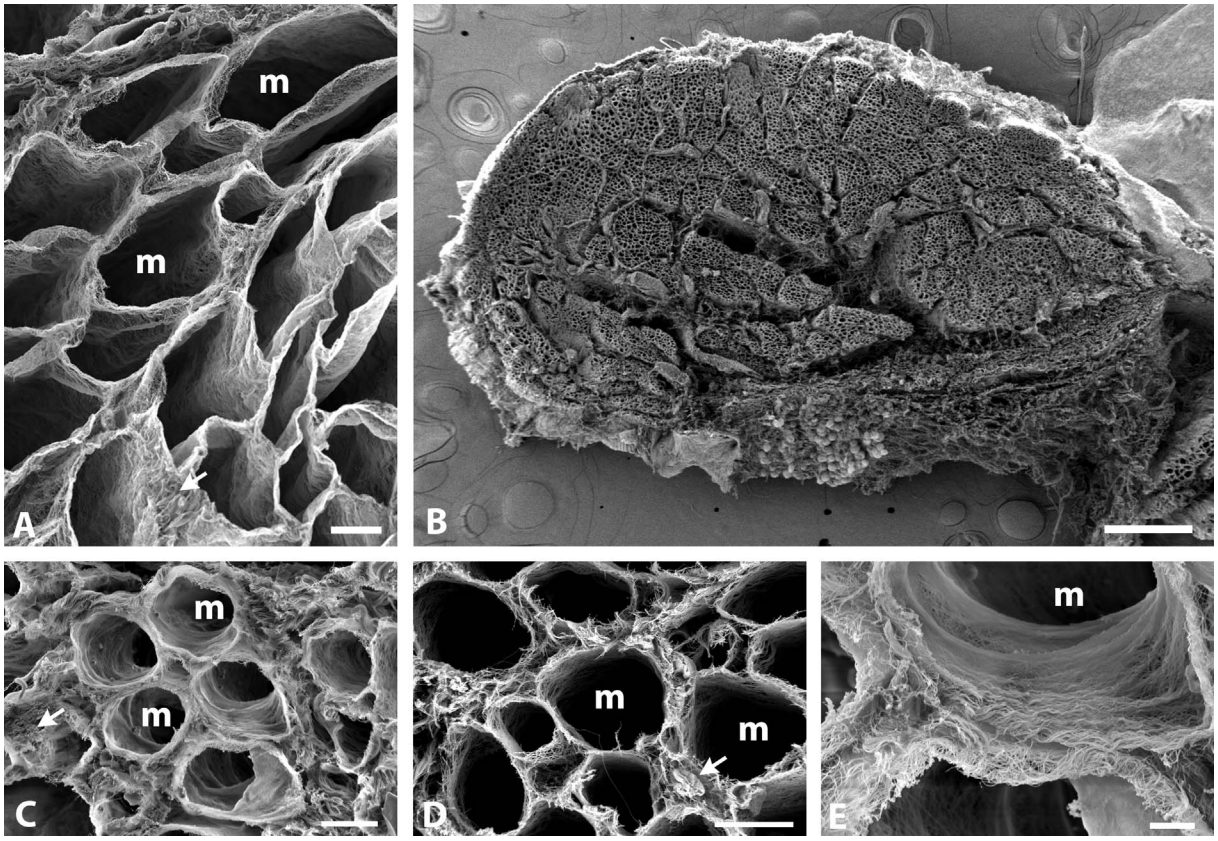

FIGURE 3. (**A–E**) Scanning electron micrographs of rabbit gastrocnemius muscle (**A**) and human medial rectus (**B–E**). Notice that myofibers (m; here seen as the tubular cavities corresponding to the digested myofibers) in the limb muscle share the connective tissue sleeve forming the endomysium with the adjacent myofibers. The whole EOM cross section shows the impressive connective tissue network interconnecting both layers and extending all the way from the fibers to the perimysium and the epimysium (**B**). At higher magnifications (**C–E**), a very generous network of curvilinear fibrils surrounds each myofiber (m) separately (**C**) or as a common boundary between adjacent myofibers (**D**). The network widely anchors the myofibers across the interstitial space between them and extends to the perimysium (*arrows*). *Scale bars*: 20 μm (**A**), 500 μm (**B**), 10 μm (**C**, **D**), 2 μm (**E**).

individual myofibers, spanning between individual myofibers, and running both circumferentially and longitudinally, in a heterogeneous fashion, within and along the length of the EOMs (Fig. 2E).

Connective Tissue Architecture

In order to better assess the connective tissue content in its entirety, human and rabbit EOMs, as well as rabbit leg muscle, were prepared for scanning electron microscopic examination. A well-established protocol was used, and the rabbit leg muscles exhibited a morphology similar to the muscles previously examined by this method.[31] Tubular cavities corresponding to the digested myofibers were surrounded by a continuous network of fibrils forming the endomysium, perimysium, and epimysium, closely connecting the adjacent myofibers, fascicles, and muscles (Fig. 3A). Scanning electron microscopic examination of the EOMs revealed the impressive magnitude of connective tissue (Fig. 3B) with clearly evident continuity between the orbital and global layers. A generous network of connective tissue extended from the myofiber surfaces to the interstitial space and perimysium. Each individual myofiber either had an independent connective tissue sleeve (Fig. 3C) or it shared part of its sleeve with other, immediately adjacent myofibers (Fig. 3D) in a fashion more similar to that of limb muscle fibers (Fig. 3A). At high magnification, the endomysium appeared as a well-organized continuous network of curvilinear fibrils closely surrounding the muscle fibers and extending into the perimysial spaces (Fig. 3E). These interconnected fibrils were seen to run the full length of the EOMs, run the full thickness of the EOMs, and attach to the epimysial connective tissue fibrils surrounding the entire muscle (Fig. 3B).

Physiological Assessment of Lateral Force Transmission

The contention that there are separate compartments that act differently from each other, whether orbital versus global or lateral versus medial, is not supported by this extensive connective tissue connectedness. These connections suggest that lateral dissipation of contractile force must also occur in the EOMs. Rabbit superior rectus muscles, dissected from scleral tendon to apex, were removed with the entire epimysium intact. In every pair of muscles examined, measurable force was produced in the lateral orientation (Fig. 4). The measured force in the lateral direction increased proportionally with the increased longitudinal force at each of the increased increments of stimulation frequency. The lateral force was significantly less than the force generated in the longitudinal direction, but the percent difference was proportional at all stimulation frequencies. It was also easily measured in all EOMs examined.

Investigative Ophthalmology & Visual Science

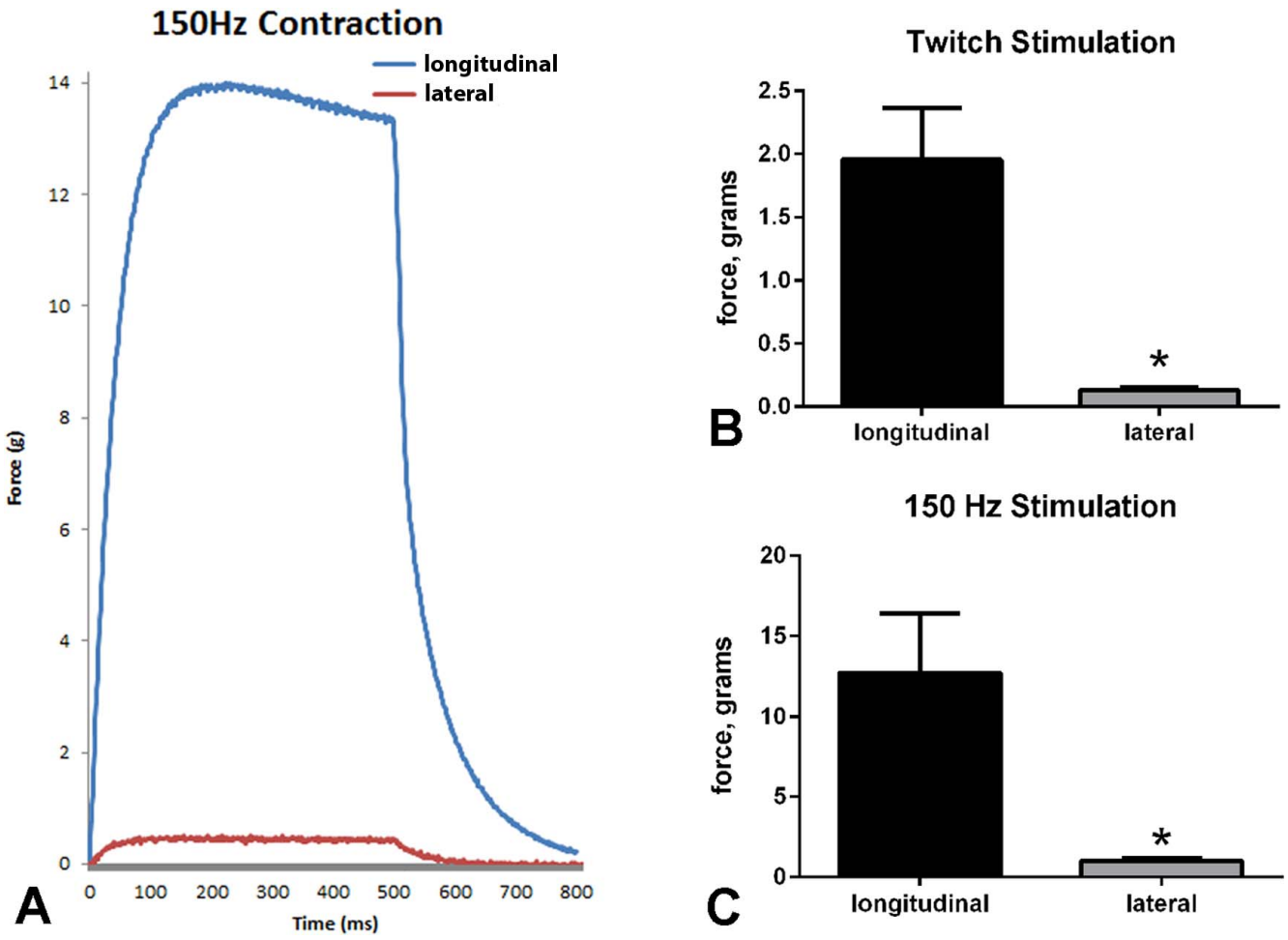

FIGURE 4. (**A**) Example of the force in grams of one muscle stimulated at 150 Hz. The *blue trace* is in the longitudinal orientation, and the *red trace* depicts force in the medial to lateral (lateral) dimension. (**B**) Mean force in grams after a single twitch stimulation ($n = 4$). *Significant difference from the force generated in the longitudinal direction. (**C**) Mean force in grams after a 150-Hz stimulation ($n = 4$). *Significant difference from the force generated in the longitudinal direction.

DISCUSSION

In all the EOMs examined, significant connective tissue ensheathments were seen around the individual fibers, between the individual fibers in the interstitial space, in the perimysium, and between the perimysium and the epimysium surrounding the whole muscles. This significant interconnectedness was apparent with both the immunohistochemical examination of individual connective tissue components and in the scanning electron micrographs. The functional consequences of these extensive interconnections were seen electrophysiologically in the demonstration of proportionally increasing lateral force dissipation when the intact EOMs were stimulated in vitro.

The patterns of localization of the various connective tissue elements in the human adult EOMs were similar to those seen in a study of collagen and elastin in human pediatric muscles.[33] These connective tissue elements are known to play a critical role in bearing the passive load during muscle contraction and define the tensile properties of skeletal muscle function.[34] The collagen protein profile has been shown to respond to activity, which in turn was demonstrated to modify the mechanical and viscoelastic properties of the exercised muscles.[35] Conversely, diseases such as Graves' ophthalmopathy resulted in significant fibrosis within individual EOMs[36] and significantly decreased range of motion.[37] Collagens and elastin were also shown to be up-regulated in subjects with strabismus and modulated after strabismus surgery.[33] Not only do these studies all point to the importance of the connective tissue within skeletal muscles but also its potential adaptations in aging and disease.

The presence of these extensive interfiber connective tissue elements is well described for limb skeletal muscles.[11,31,38] This phenomenon was clearly demonstrated for muscles with multiple heads where direct force transmission was experimentally prevented at one or more of the insertional heads.[39] In this case, force transmission occurred laterally from the tenotomized to the intact heads and required intact perimysial and epimysial connective tissues for this transfer of force. Even more compelling was the demonstration that lengthening of the tibialis anterior or peroneal muscle groups significantly reduced force in the distal extensor digitorum longus,[40,41] as did shortening one head of the extensor digitorum longus,[42] again only when connective tissue ensheathments were intact.[43,44] It is interesting that myofascial or lateral force transmission was shown to be more significant when the muscle produced lower forces,[18] which supports its critical importance in eye movements, which are considered to be low-force movements. The lateral transmission of force is considered to be functionally important, particularly for muscles with short, in-series muscle fibers with tapered intrafascicular terminations.[14,16,17,45] This type of overlapping arrangement of short fibers is present in the EOMs[3–5] and

supports the view that these lateral connections between fibers and between muscle fascicles is a critical component of force transmission when muscle contractions occur during eye movements.

Neurophysiological examination of abducens motor neuron activity while simultaneously measuring lateral rectus muscle force showed that motor units in the ocular motor nuclei are nonadditive.[46–48] The summed forces of individual motor units are far higher than the force actually measured when the whole nerve was stimulated. The significant loss of force in the EOM experiments when the whole nerve was stimulated is evidence of polyinnervation but was also postulated to be due to the serial and branching arrangement of muscle fibers in the EOMs, as well as the interfiber connective tissue matrix.[46] Our ability to measure this lateral force component further emphasizes the important functional role the interconnected endomysial, perimysial, and epimysial connective tissue elements play in normal EOM function.

The hypothesis that different parts of the EOMs can move independently is at odds with the significant interconnectedness of the connective tissue elements with all the muscle fibers along the whole length of all skeletal muscle, including direct connection into the epimysium. It is likely that compartmental movements that were considered minor were due to the complete removal of the epimysium in the preparation used in those studies, where exposed muscle fibers are evident in the figures.[26] Removal of the epimysium would disrupt the normally robust connections of this layer with the perimysium and endomysium. In the studies describing active contraction, again, the epimysium was removed, disrupting the normal connective tissue anatomical connections.[27]

In summary, the EOMs contain a significant amount of connective tissue composed of a complex mixture of fibrillar proteins. These fibrils interconnect individual myofibers, myofibers within fascicles, as well as connect each fascicle with the epimysium that covers the muscles from tendon to apex. During eye movements, these interconnected connective tissue elements produce a significant lateral dissipation of muscle force particularly meaningful for these low-force movements. Collectively, these data support the view that the connective tissue is highly interconnected. This strongly suggests that individual isolated movements of compartments within the EOM are unlikely. As the connective tissue elements are strongly interconnected from the endomysium, through the perimysium with no interruption from the global through the orbital layer and into the surrounding epimysium, it is unlikely that independent movements occur within the EOM.

Acknowledgments

The authors thank the Cheng Choo Nikki Lee for technical assistance and the facilities of the Umeå Core Facility Electron Microscopy (UCEM) at the Chemical Biological Centre (KBC), Umeå University.

Supported by grants from the Swedish Research Council (2015-02438; Stockholm, Sweden), County Council of Västerbotten (Umeå, Sweden), Ögonfonden (Umeå, Sweden), Kronprinsessan Margaretas Arbetsnämnd för Synskadade (Valdemarsvik, Sweden), and The Medical Faculty, Umeå University (Umeå, Sweden); National Eye Institute Grant RO1 EY15313 (LKM), NIH grant P30 EY11375, the Minnesota Lions Foundation, and an unrestricted grant to the Department of Ophthalmology from Research to Prevent Blindness, Inc.

Disclosure: **L.K. McLoon**, None; **A. Vicente**, None; **K.R. Fitzpatrick**, None; **M. Lindström**, None; **F. Pedrosa Domellöf**, None

References

1. Kjellgren D, Thornell LE, Andersen J, Pedrosa-Domellöf F. Myosin heavy chain isoforms in human extraocular muscles. *Invest Ophthalmol Vis Sci*. 2003;44:1419–1425.
2. McLoon LK, Willoughby CL, Andrade FH. Extraocular muscles: structure and function. In: McLoon LK, Andrade FH, eds. *Craniofacial Muscles: A New Framework for Understanding the Effector Side of Craniofacial Muscles*. Basel, Switzerland: Springer; 2012:31–88.
3. Mayr R. Structure and distribution of fibre types in the external eye muscles of the rat. *Tissue Cell*. 1971;3:433–462.
4. Alvarado-Mallart RM, Pincon-Raymond M. Nerve endings on the intramuscular tendons of cat extraocular muscles. *Neurosci Lett*. 1976;2:121–125.
5. Harrison AR, Anderson BC, Thompson LV, McLoon LK. Myofiber length and three-dimensional localization of NMJs in normal and botulinum toxin treated adult extraocular muscles. *Invest Ophthalmol Vis Sci*. 2007;48:3594–3601.
6. Cheng G, Merriam AP, Gong B, Leahy P, Khanna S, Porter JD. Conserved and muscle-group-specific expression patterns shape postnatal development of the novel extraocular muscle phenotype. *Physiol Genomics*. 2004;18:184–195.
7. Kjellgren D, Thornell LE, Virtanen I, Pedrosa-Domellöf F. Laminin isoforms in human extraocular muscles. *Invest Ophthalmol Vis Sci*. 2004;45:4233–4239.
8. Kusner LL, Young A, Tjoe S, Leahy P, Kaminski HJ. Perimysial fibroblasts of extraocular muscle, as unique as the muscle fibers. *Invest Ophthalmol Vis Sci*. 2010;51:192–200.
9. Nyström A, Holmblad J, Pedrosa Domellöf F, Sasaki T, Durbeej M. Extraocular muscle is spared upon complete laminin alpha2 chain deficiency: comparative expression of laminin and integrin isoforms. *Matrix Biol*. 2006;25:382–385.
10. Liu JX, Brännström T, Andersen PM, Pedrosa Domellöf F. Different impact of ALS on laminin isoforms in human extraocular muscles versus limb muscles. *Invest Ophthalmol Vis Sci*. 2011;52:4842–4852.
11. Rowe RWD. Morphology of perimysial and endomysial connective tissue in skeletal muscle. *Tissue Cell*. 1981;13:681–690.
12. Purslow PP. Strain-induced reorientation of an intramuscular connective tissue network: implications for passive muscle elasticity. *J Biomech*. 1989;22:21–31.
13. Trotter JA. Functional morphology of force transmission in skeletal muscle. *Acta Anat*. 1993;146:205–222.
14. Huijing PA. Muscle as a collagen fiber reinforced composite: a review of force transmission in muscle and whole limb. *J Biomech*. 1999;32:329–345.
15. Kjaer M. Role of extracellular matrix in adaptation of tendon and skeletal muscle to mechanical loading. *Physiol Rev*. 2004;84:649–698.
16. Boriek AM, Zhu D, Zeller M, Rodarte JR. Inferences on force transmission from muscle fiber architecture of the canine diaphragm. *Am J Physiol Regul Integr Comp Physiol*. 2001;280:R156–R165.
17. Harris AJ, Duxson MJ, Butler JE, Hodges PW, Taylor JL, Gandevia SC. Muscle fiber and motor unit behavior in the longest human skeletal muscle. *J Neurosci*. 2005;25:8528–8533.
18. Meijer HJM, Baan GC, Huijing PA. Myofascial force transmission is increasingly important at lower forces: firing frequency-related length-force characteristics of rat extensor digitorum longus. *Acta Physiol*. 2006;186:185–195.
19. Duance VC, Restall DJ, Beard H, Bourne FJ, Bailey AJ. The location of three collagen types in skeletal muscle. *FEBS Lett*. 1977;79:248–252.

20. Foidart M, Foidart JM, Engel WK. Collagen localization in normal and fibrotic human skeletal muscle. *Arch Neurol*. 1981;38:152–157.
21. Irwin WA, Bergamin N, Sabatelli P, et al. Mitochondrial dysfunction and apoptosis in myopathic mice with collagen VI deficiency. *Nature Genet*. 2003;35:367–371.
22. Muiznieks LD, Weiss AS, Keeley FW. Structural disorder and dynamics of elastin. *Biochem Cell Biol*. 2010;88:239–250.
23. Ushiki T. Collagen fibers, reticular fibers and elastic fibers. A comprehensive understanding from a morphological viewpoint. *Arch Histol Cytol*. 2002;65:109–125.
24. Engler AJ, Rehfeldt F, Sen S, Discher DE. Microtissue elasticity: measurements by atomic force microscopy and its influence on cell differentiation. *Methods Cell Biol*. 2007;83:521–545.
25. Lim KH, Poukens V, Demer JL. Fascicular specialization in human and monkey rectus muscles: evidence for anatomic independence of global and orbital layers. *Invest Ophthalmol Vis Sci*. 2007;48:3089–3097.
26. Shin A, Yoo L, Chaudhuri Z, Demer JL. Independent passive mechanical behavior of bovine extraocular muscle compartments. *Invest Ophthalmol Vis Sci*. 2012;53:8414–8423.
27. Shin A, Yoo L, Demer JL. Independent active contraction of extraocular muscle compartments. *Invest Ophthalmol Vis Sci*. 2014;56:199–206.
28. Kovanen V. Intramuscular extracellular matrix: complex environment of muscle cells. *Exerc Sport Sci Rev*. 2002;30:20–25.
29. Gelse K, Poschl E, Aigner T. Collagens–structure, function, and biosynthesis. *Adv Drug Deliv Rev*. 2003;55:1531–1546.
30. Ricard-Blum S, Ruggiero F. The collagen superfamily: from the extracellular matrix to the cell membrane. *Pathol Biol (Paris)*. 2005;53:430–442.
31. Trotter JA, Purslow PP. Functional morphology of the endomysium in series fibered muscles. *J Morphol*. 1992;212:109–122.
32. Anderson BC, Christiansen SP, Grandt S, Grange RW, McLoon LK. Increased extraocular muscle strength with direct injection of insulin-like growth factor-I. *Invest Ophthalmol Vis Sci*. 2006;47:2461–2467.
33. Stager D Jr, McLoon LK, Felius J. Postulating a role for connective tissue elements in inferior oblique muscle overaction. (An American Ophthalmological Society Thesis). *Trans Am Ophthalmol Soc*. 2013;111:119–132.
34. Brown SH, Carr JA, Ward SR, Lieber RL. Passive mechanical properties of rat abdominal wall muscles suggest an important role of the extracellular connective tissue matrix. *J Orthop Res*. 2012;30:1321–1326.
35. Kjaer M, Magnusson P, Krogsgaard M, et al. Extracellular matrix adaptation of tendon and skeletal muscle to exercise. *J Anat*. 2006;208:445–450.
36. Eckstein AK, Johnson KT, Thanos M, Esser J, Ludgate M. Current insights into the pathogenesis of Graves' ophthalmopathy. *Horm Metab Res*. 2009;41:456–464.
37. Fishman DR, Benes SC. Upgaze intraocular pressure changes and strabismus in Graves' ophthalmopathy. *J Clin Neuroophthalmol*. 1991;11:162–165.
38. Passerieux E, Rossignol R, Letellier T, Delage JP. Physical continuity of the perimysium from myofibers to tendons: Involvement in lateral force transmission in skeletal muscle. *J Struct Biol*. 2007;159:19–28.
39. Huijing PA, Baan GC, Rebel GT. Non-myotendinous force transmission in rat extensor digitorum longus muscle. *J Exp Biol*. 1998;201:682–691.
40. Maas H, Jaspers RT, Baan GC, Huijing PA. Myofascial force transmission between a single muscle head and adjacent tissues: length effect of head III of rat EDL. *J Appl Physiol*. 2003;95:2004–2013.
41. Huijing PA, van de Langenberg RW, Meesters JJ, Baan GC. Extramuscular myofascial force transmission also occurs between synergistic muscles and antagonistic muscles. *J Electromyogr Kinesiol*. 2007;17:680–689.
42. Maas H, Huijing PA. Myofascial force transmission in dynamic muscle conditions: effects of dynamic shortening of a single head of multi-tendoned rat extensor digitorum longus muscle. *Eur J Appl Physiol*. 2005;94:584–592.
43. Huijing PA, Maas H, Baan GC. Compartmental fasciotomy and isolating a muscle from neighboring muscles interfere with myofascial force transmission within the rat anterior crural compartment. *J Morphol*. 2003;256:306–321.
44. Huijing PA, Baan GC. Myofascial force transmission: muscle relative position and length determine agonist and synergist muscle force. *J Appl Physiol*. 2003;94:1092–1107.
45. Trotter JA. Interfiber tension transmission in series-fibered muscles of the cat hindlimb. *J Morphol*. 1990;206:351–361.
46. Goldberg SJ, Wilson KE, Shall MS. Summation of extraocular motor unit tensions in the lateral rectus muscle of the cat. *Muscle Nerve*. 1997;20:1229–1235.
47. Goldberg SJ, Meredith MA, Shall MS. Extraocular motor unit and whole-muscle response in the lateral rectus muscle of the squirrel monkey. *J Neurosci*. 1998;18:10629–10639.
48. Miller JM, Davison RC, Gamlin PD. Motor nucleus activity fails to predict extraocular muscle forces in ocular convergence. *J Neurophysiol*. 2011;105:2863–2873.

Investigative Ophthalmology & Visual Science